1276 KSME International Journal, Vol. 16 No. 10, pp. 1276~1286, 2002

Analysis of Static and Dynamic Frictional Contact of Deformable Bodies Including Large Rotations of the Contact Surfaces

Kisu Lee*

Department of Mechanical Engineerin, Chonbuk National University, Chon Ju, Chonbuk 561-756, Korea

The numerical techniques are presented to solve the static and dynamic contact problems of deformable bodies having large rotations of the contact surfaces. The contact conditions on the possible contact surfaces are enforced by using the contact error vector, and an iterative scheme similar to augmented Lagrange multiplier method is employed to reduce the contact error vector monotonically. For dynamic contact problems using implicit time integration, a contact error vector is also defined by combining the displacement, velocity, and acceleration on the contact surface. The suggested iterative technique is implemented to ABAQUS by using the UEL subroutine UEL. In this work, after the computing procedures to solve the frictional contact problems are explained, the numerical examples are presented to compare the present solutions with those obtained by ABAQUS.

Key Words : Frictional Contact, Dynamic Contact, Differential Algebraic Equations, Stability of the Solution

1. Introduction

Accurate analysis of contact problem is important in many engineering fields. For example, wear analysis requires correct contact stress distribution, and solution for the dynamics of rotating movements usually requires correct contact force between them. Even though the numerical techniques such as Lagrange multiplier method and penalty method are widely used to solve any kind of contact problems in the finite element codes, it is well known that they usually have shortcomings in the computational stability or the accuracy of the solution if the model is complicated. For example the ill-conditioned or non-symmetric matrices usually appear in the global equations, and thus the convergence and accuracy of the Newton Raphson iterations of the global equations face numerical difficulties. Such numerical difficulties generally become severe if the possible contact surfaces experience large rotations because of the complicated contact constraints involving the normal direction change on the contact surfaces. Due to such numerical difficulties, the numerical solution of contact problems having large rotations of contact surfaces usually involves spurious oscillations. Even though various elaborate solution techniques for the contact problems associated with large deformation have been suggested in the literature (e.g., Ghosh (1992) Heegaard and Curnier (1993) and Laursen and Simo (1993)), such divergence and oscillations occur due to many reasons, and it is practically impossible to make a general-purpose program which is free of such numerical instabilities for all cases. Thus, it would be very convenient if a user can develop a special contact analysis program which is most appropriate for a specific problem by using a user subroutine of a commercial program. However, due to the diversity and complexity of the contact analysis

* **E-mail** : kisulee@moak.chonbuk.ac.kr
TEL : +82-63-270-2326; **FAX** : +82-63-270-2315
Department of Mechanical Engineerin, Chonbuk National University, Chon Ju, Chonbuk 561-756, Korea. (Manuscript **Received** October 8, 2001; **Revised** July 8, 2002)

techniques, there can be no user subroutine in the commercial codes which can be directly used for any type of contact analysis by the user. For example, even though ABAQUS 6.2 (2001) newly introduced the user subroutine UINTER to compute general surface interaction on contact surfaces, it is difficult to use UINTER for the contact analysis based on augmented Lagrange multiplier method or point-to-point contact for dynamics problems.

In this work, it is shown that the contact problems of nonlinearly deformable bodies having large rotations on the contact surfaces can be solved by using the iterative scheme and contact error vector of Lee (1989). To systematically impose all the contact conditions on the iterative scheme, the contact error vector is defined by using the contact conditions on the possible contact surfaces, and the contact error vector is monotonically reduced toward zero by the iterative scheme. By this way all the contact conditions on any possible contact point can be automatically satisfied by the iterative scheme. The basic computing procedure at each iteration of this work consists of the two steps similar to those of augmented Lagrange multiplier method (see, e.g., Crisfield (1997) for augmented Lagrange multiplier method). The first step is to compute the contact force by using the contact error vector determined on the geometry of the previous iteration, and the second step is to compute the contact error vector after solving the global equilibrium equation with the given contact force. This simple iterative scheme does not produce any ill-conditioned or nonsymmetric matrix, and thus an accurate solution may be obtained with good computational stability. Also, in this work, it is shown that dynamic contact problem is solved by the present iterative scheme by using a contact error vector consisting of the displacement, velocity, and acceleration of the contact points.

Especially, in this work, the presented techniques for contact analysis are implemented to ABAQUS by using the user subroutine UEL of ABAQUS. Thus, even though all the contact constraints on the possible contact surfaces are imposed by using the user subroutine UEL of ABAQUS, all the other FEM computations concerning the deformations of the solids are conveniently performed by ABAQUS. In this work, after the computing procedures to solve the frictional contact problems are explained, the numerical examples are presented to compare the present solutions with those solved by ABAQUS.

2. Contact Condition

In this work, two-dimensional bodies experiencing large deformations are considered and the standard finite element techniques are employed. Especially, in the equations of equilibrium, the contact force is assumed to be known before the solution That is, the contact force is treated as a prescribed external force in the equations of equilibrium, and its correct value is determined by the iterative scheme explained later. Also an implicit time integration technique is used in the case of dynamics problems. Then, by the equations of equilibrium, at time step $t+\Delta t$, the relation between the displacement and the contact force on the contact pairing surfaces A and B may be written as

$$\begin{aligned} \delta(\mathbf{u}^A)^{t+\Delta t} &= \delta(\mathbf{w}^A)^{t+\Delta t} + (\mathbf{C}^A)^{t+\Delta t}\delta\mathbf{p}^{t+\Delta t} \\ \delta(\mathbf{u}^A)^{t+\Delta t} &= \delta(\mathbf{w}^B)^{t+\Delta t} - (\mathbf{C}^B)^{t+\Delta t}\delta\mathbf{p}^{t+\Delta t} \end{aligned} \tag{1}$$

where $\mathbf{u}$ is the displacement on the possible contact surface due to all the forces including the contact force, $\mathbf{w}$ is the displacement on the possible contact surface due to the forces except the contact force, $\mathbf{p}$ is the contact force, and $\mathbf{C}$ is the matrix relating the contact force and the displacement. Also, δ denotes the small change, and superscripts A and B denote surfaces A and B, respectively. Especially, in Eq. (1), all the vectors $\mathbf{u}$, $\mathbf{w}$, and $\mathbf{p}$ are written in terms of the normal and tangential components.

In this work, at each time step, after giving the value of contact force $\mathbf{p}$ by the iterative scheme which will be explained in the next section, displacement $\mathbf{u}$ is computed by solving the global equations of equilibrium. Since the global equi-

librium equations are nonlinear in large deformation problems, Newton Raphson method is generally used to solve them. Whenever displacement u is computed at each iteration of each time step, the contact pairing points and the normal directions are determined by drawing the normal lines from the nodal points on the possible contact surface of a body to the possible contact surface of the other body. Similar to ABAQUS which uses the master and slave surfaces, to draw the normal lines, the possible contact surfaces are made to be smooth by the polynomial interpolations using the geometry of several nodal points adjacent to the contact points. Now let $p_{i\eta}$ and $p_{i\ell}$ denote the normal and tangential contact forces at contact point i, $s_{i\eta}$ denote the normal penetration at point i, $s_{i\ell}$ denote the incremental relative tangential sliding at point i, and μ denote the friction coefficient of Coulomb friction law. Then the contact condition at point i at time step $t+\Delta t$ may be written as

$$\begin{aligned}
&p_{i\eta}^{t+\Delta t}\le 0\\
&s_{i\eta}^{t+\Delta t}\le 0\\
&p_{i\eta}^{t+\Delta t}=0 \text{ if } s_{i\eta}^{t+\Delta t}<0\\
&s_{i\ell}^{t+\Delta t}=0 \text{ if } |p_{i\ell}^{t+\Delta t}|<\mu |p_{i\eta}^{t+\Delta t}|\\
&s_{i\ell}^{t+\Delta t}=-\beta p_{i\ell}^{t+\Delta t} \text{ with some value of } \beta(\beta\ge 0)\\
&\qquad \text{if } |p_{i\ell}^{t+\Delta t}|=\mu |p_{i\eta}^{t+\Delta t}|>0
\end{aligned} \tag{2}$$

From the above contact condition, at time step $t+\Delta t$, for the iterative scheme of this work, contact error vector $\mathbf{v}^{t-\Delta t}$ is defined as

$$\begin{aligned}
&v_{i\eta}^{t+\Delta t}=s_{i\eta}^{t+\Delta t} \text{ if } p_{i\eta}^{t+\Delta t}<0 \text{ or } s_{i\ell}^{t+\Delta t}>0\\
&\quad =0 \text{ otherwise}\\
&v_{i\ell}^{t+\Delta t}=s_{i\ell}^{t+\Delta t} \text{ if } |p_{i\ell}^{t+\Delta t}|<\tau_i^{t+\Delta t}\\
&\qquad \text{or } \{\operatorname{sign}(p_{i\ell}^{t+\Delta t})=\operatorname{sign}(s_{i\ell}^{t+\Delta t}) \text{ and } \tau_i^{t+\Delta t}>0\}\\
&\quad =0 \text{ otherwise}
\end{aligned} \tag{3}$$

where $\tau_i^{t+\Delta t}$ is the maximum frictional force at point i defined as

$$\tau_i^{t+\Delta t}=\mu |p_{i\eta}^{t+\Delta t}| \tag{4}$$

Then contact condition (2) can be written as

$$\begin{aligned}
&p_{i\eta}^{t+\Delta t}\le 0\\
&|p_{i\ell}^{t+\Delta t}|\le \tau_i^{t+\Delta t}\\
&\mathbf{v}^{t+\Delta t}=\mathbf{0}
\end{aligned} \tag{5}$$

3. Solution Method

3.1 Iterative scheme

This work uses the iterative scheme similar to the augmented Lagrange multiplier method, and the computation at each iteration consists of two major steps: the first step is to compute the contact force by using the contact error vector of the previous iteration, and the second step is to solve the global equilibrium equations and to compute the contact error vector of the current iteration. Since displacement $\mathbf{u}$ is determined by solving the global equilibrium equations after the contact force is given, if the correct value of the contact force is given before solving the global equilibrium equations, contact condition (2) is automatically satisfied on the possible contact points by the solution of the global equilibrium equations. Thus, in this work, the correct value of contact force $\mathbf{p}^{t+\Delta t}$ at time step $t+\Delta t$ is determined by monotonically reducing the contact error $\mathbf{v}^{t+\Delta t}$ by using the following iterative scheme of Lee (1989):

$$\begin{aligned}
&\begin{bmatrix}\bar{p}_{i\eta}^{t+\Delta t,m}\\ \bar{p}_{i\ell}^{t+\Delta t,m}\end{bmatrix}=\begin{bmatrix}p_{i\eta}^{t+\Delta t,m-1}\\ p_{i\ell}^{t+\Delta t,m-1}\end{bmatrix}-\alpha\begin{bmatrix}s_{i\eta}^{t-\Delta t,m-1}\\ s_{i\ell}^{t+\Delta t,m-1}\end{bmatrix}\\
&p_{i\eta}^{t+\Delta t,m}=\min(\bar{p}_{i\eta}^{t+\Delta t,m},\ 0)\\
&p_{i\ell}^{t+\Delta t,m}=\operatorname{sign}(\bar{p}_{i\ell}^{t+\Delta t,m})\min(|\bar{p}_{i\ell}^{t+\Delta t,m}|,\ \tau_i^{t+\Delta t})\\
&\qquad \text{if } v_{i\ell}^{t+\Delta t,m-1}=s_{i\ell}^{t+\Delta t,m-1}\\
&\quad =\operatorname{sign}(\bar{p}_{i\ell}^{t+\Delta t,m})\,\tau_i^{t+\Delta t} \text{ if } v_{i\ell}^{t+\Delta t,m-1}=0\ne s_{i\ell}^{t+\Delta t,m-1}
\end{aligned} \tag{6}$$

In the above iterative scheme, m denotes the iteration counter, α is a scalar number which will be explained later, and $s_{i\eta}^{t+\Delta t,m-1}$ and $s_{i\ell}^{t+\Delta t,m-1}$ denote the value of $s_{i\eta}^{t+\Delta t}$ and $s_{i\ell}^{t+\Delta t}$ computed by the solution of the global equilibrium equation using $p_{i\eta}^{t+\Delta t,m-1}$ and $p_{i\ell}^{t+\Delta t,m-1}$ as the contact forces. Also, $v_{i\ell}^{t+\Delta t,m-1}$ denotes the tangential component of the contact error defined by (3) using $p_{i\eta}^{t+\Delta t,m-1}$, $p_{i\ell}^{t+\Delta t,m-1}$, $s_{i\eta}^{t+\Delta t,m-1}$, and $s_{i\ell}^{t+\Delta t,m-1}$. $\tau_i^{t+\Delta t}$ is computed as $\tau_i^{t+\Delta t}=\mu|p_{i\eta}^{t+\Delta t}|$ with prescribed normal contact force $p_{i\eta}^{t+\Delta t}$. In the real computing procedure, as explained in the next section, $p_{i\eta}^{t+\Delta t}$ is revised several times in time step $t+\Delta t$ until $p_{i\eta}^{t+\Delta t}$ becomes almost equal to $p_{i\eta}^{t+\Delta t,m-1}$ in the above iterative scheme. With the displacement computed at each iteration, the contact pairing points and

the normal directions are determined at each iteration of this procedure by drawing the normal lines from the nodal points on the contact surface of a body to the pairing contact surface of the other body. Also, with the contact forces given by the above iterative scheme, the global equilibrium equations are solved at each iteration of this procedure and the corresponding contact error vector is computed by Eq. (3) on the possible contact surface.

Dynamic contact problems bring additional difficulties in the numerical solution. Traditionally, in the dynamic contact analysis using finite element techniques, most of the researchers revised the velocities of the contact points by introducing the momentum balance of the contact points without simultaneously solving the global equations of motion (e.g., Hughes et al. (1976), Bathe and Chaudhary (1986), and ABAQUS (2001)). Then, even though the velocities on the contact surface might agree with those of the mating contact surface, the velocities on the contact surface are not consistently derived from the velocity field inside the continuous solid, and this may result in numerical oscillations in the solution. To the author's best knowledge the difficulties in the solution of dynamic contacts occur mainly because the equations of motion are differential equations while the contact constraints are algebraic constraints. For example, if any point sustains normal contact and tangential sticking in a series of consecutive time steps, the contact conditions on this point are expressed by the algebraic equations without any inequality constraint. Thus the differential algebraic equations consisting of the equations of motion and the contact constraint should be solved simultaneously (see, e.g., Petzold (1982) for differential algebraic equations). Also, the spurious high-frequency oscillations which usually appear in the dynamic contact analysis may be almost prevented by introducing the solution strategies of the differential algebraic equations which also consider the differentiated terms of the contact constraints (Taylor and Papadopoulos (1993) and Lee (1994, 1997)). For this reason, to impose the differentiated constraints on the contact points by using the UEL subroutine of ABAQUS, the following contact error vector is defined for the dynamic contact by combining the displacement and velocity of the contact point:

$$
\begin{aligned}
v_i^{t+\Delta t} &= s_i^{t+\Delta t} \text{ if } \left[p_i^{t+\Delta t}<0 \text{ or } s_i^{t+\Delta t}>0\right] \text{ and } p_i^t=0\\
&= \left(s_i^{t+\Delta t}+\beta \dot{s}_i^{t+\Delta t}\Delta t+\gamma \ddot{s}_i^{t+\Delta t}\Delta t^2\right)/3\\
&\quad \text{if } \left[p_i^{t+\Delta t}<0 \text{ or } s_i^{t+\Delta t}+\beta \dot{s}_i^{t+\Delta t}\Delta t+\gamma \ddot{s}_i^{t+\Delta t}\Delta t^2>0\right] \text{ and } p_i^t<0\\
&= 0 \text{ otherwise}\\
v_i^{t+\Delta t} &= s_i^{t+\Delta t} \text{ if } \left[|p_i^{t+\Delta t}|<\mu^{t+\Delta t}\right.\\
&\quad \left. \text{or } \left\{\text{sign}(p_i^{t+\Delta t})=\text{sign}(s_i^{t+\Delta t}>0\right\} \text{ and } \mu^{t+\Delta t}>0\right] \text{ and } p_i^t=0\\
&= \left(s_i^{t+\Delta t}+\beta \dot{s}_i^{t+\Delta t}\Delta t+\gamma \ddot{s}_i^{t+\Delta t}\Delta t^2\right)/3\\
&\quad \text{if } \left[|p_i^{t+\Delta t}|<\mu^{t+\Delta t} \text{ or } \left\{\text{sign}(p_i^{t+\Delta t})=\text{sign}(s_i^{t+\Delta t}+\beta \dot{s}_i^{t+\Delta t}\Delta t\right.\right.\\
&\qquad \left.\left. +\gamma \ddot{s}_i^{t+\Delta t}\Delta t^2) \text{ and } \mu^{t+\Delta t}>0\right\}\right] \text{ and } p_i^t<0\\
&= 0 \text{ otherwise}
\end{aligned}
\tag{7}
$$

In the above equation, β and γ are weight factors and $v_i^{t+\Delta t}$ and $v_i^{t+\Delta t}$ become different from those of Eq. (3) if point i experienced contact in the previous time step (i.e., if $p_i^t<0$). With the contact error defined as above, if $s_i^{t+\Delta t,m-1}$ and $\dot{s}_i^{t+\Delta t,m-1}$ are replaced by $(s_i^{t+\Delta t,m-1}+\beta \dot{s}_i^{t+\Delta t,m-1}\Delta t+\gamma \ddot{s}_i^{t+\Delta t,m-1}\Delta t^2)/3$ and $(\dot{s}_i^{t+\Delta t,m-1}+\beta \ddot{s}_i^{t+\Delta t,m-1}\Delta t+\gamma \dddot{s}_i^{t+\Delta t,m-1}\Delta t^2)/3$ at point i of $p_i^t<0$, iterative scheme given by Eq. (6) is used again for dynamic contact analysis of this work.

3.2 Explanation on the convergence of the iterative scheme

In this section the monotone reduction of the error vector of Eq. (3) by the iterative scheme given by Eq. (6) is explained. The same theory is applied even if the contact error vector of Eq. (7) is used instead of the contact error vector of Eq. (3) because, as long as Δt is small, δs is proportional to $\delta \dot{s} \Delta t$. As the present method is essentially the same as that of Lee (1989, 1994), only a brief explanation is given here. Assuming a small value of α in Eq. (6), the changes in the normal directions of the contact points become negligible. Then, as s denotes the penetration, the following relation can be obtained:

$$
\begin{aligned}
\mathbf{s}^{t+\Delta t,m}-\mathbf{s}^{t+\Delta t,m-1} &\approx \delta \mathbf{s}^{t+\Delta t}\\
&= \delta(\mathbf{u}^A)^{t+\Delta t}-\delta(\mathbf{u}^B)^{t+\Delta t}
\end{aligned}
\tag{8}
$$

When the displacement variation resulting from the iterative scheme given by Eq. (6) is

considered, in Eq. (1), $\delta\mathbf{u}$ is solely influenced by $\delta\mathbf{p}$. Then, assuming a small change of the contact force, the following is obtained from Eq. (1):

$$\delta(\mathbf{u}^{A})^{t+\Delta t}-\delta(\mathbf{u}^{B})^{t+\Delta t}=(\mathbf{C}^{A}+\mathbf{C}^{B})^{t+\Delta t}\delta\mathbf{p}$$
$$\approx(\mathbf{C}^{A}+\mathbf{C}^{B})^{t+\Delta t}(\mathbf{p}^{t+\Delta t,m}-\mathbf{p}^{t+\Delta t,m-1}) \quad (9)$$

From equations (8) and (9),

$$\mathbf{s}^{t+\Delta t,m}-\mathbf{s}^{t+\Delta t,m-1}$$
$$\approx(\mathbf{C}^{A}+\mathbf{C}^{B})^{t+\Delta t}(\mathbf{p}^{t+\Delta t,m}-\mathbf{p}^{t+\Delta t,m-1}) \quad (10)$$

Assuming a small value of α, from Eqs. (3), (6), and the solution of the global equilibrium equations, the following conditions can be always satisfied :

$$\begin{aligned}
&\text{if } p_{i\eta}^{t+\Delta t,m-1}<0, \text{ then } \bar{p}_{i\eta}^{t+\Delta t,m}\le 0\\
&\text{if } s_{i\eta}^{t+\Delta t,m-1}<0, \text{ then } s_{i\eta}^{t+\Delta t,m}\le 0\\
&\text{if } p_{i\ell}^{t+\Delta t,m-1}>0, \text{ then } p_{i\ell}^{t+\Delta t,m}\ge 0\\
&\text{if } p_{i\ell}^{t+\Delta t,m-1}<0, \text{ then } p_{i\ell}^{t+\Delta t,m}\le 0\\
&\text{if } s_{i\ell}^{t+\Delta t,m-1}>0, \text{ then } s_{i\ell}^{t+\Delta t,m}\ge 0\\
&\text{if } s_{i\ell}^{t+\Delta t,m-1}<0, \text{ then } s_{i\ell}^{t+\Delta t,m}\le 0\\
&\text{if } |p_{i\ell}^{t+\Delta t,m-1}|<\tau_{i}^{t+\Delta t}, \text{ then } |p_{i\ell}^{t+\Delta t,m}|\le\tau_{i}^{t+\Delta t}
\end{aligned} \quad (11)$$

If conditions in Eq. (11) are satisfied, from Eq. (6),

$$\mathbf{p}^{t+\Delta t,m}-\mathbf{p}^{t+\Delta t,m-1}=-\alpha\mathbf{s}^{t+\Delta t,m-1} \quad (12)$$

From Eqs. (10) and (12),

$$\mathbf{s}^{t+\Delta t,m}-\mathbf{s}^{t+\Delta t,m-1}=-\alpha(\mathbf{C}^{A}+\mathbf{C}^{B})^{t+\Delta t}\mathbf{S}^{t+\Delta t,m-1} \quad (13)$$

Let $\mathbf{E}$ be a diagonal matrix whose components have the value of one if the corresponding components of $\mathbf{v}^{t+\Delta t,m-1}$ are not zero, and have the value of zero if the corresponding components of $\mathbf{v}^{t+\Delta t,m-1}$ are zero. Then, if conditions of Eq. (11) are satisfied, by definition givin in Eq. (3),

$$\mathbf{E}\mathbf{s}^{t+\Delta t,m-1}=\mathbf{v}^{t+\Delta t,m-1}$$
$$\|\mathbf{v}^{t+\Delta t,m}\|_2\le\|\mathbf{E}\mathbf{s}^{t-\Delta t,m}\|_2 \quad (14)$$

Then, after multiplying the diagonal matrix $\mathbf{E}$ on the both sides of Eq. (13), the following can be obtained :

$$\|\mathbf{v}^{t+\Delta t,m}\|_2\le\|\mathbf{I}-\alpha(\mathbf{C}^{A}+\mathbf{C}^{B})^{t+\Delta t}\|_2\,\|\mathbf{v}^{t+\Delta t,m-1}\|_2 \quad (15)$$

Thus, as long as matrix $(\mathbf{C}^{A}+\mathbf{C}^{B})^{t+\Delta t}$ is positive definite (in most of the structural analysis, matrix $(\mathbf{C}^{A}+\mathbf{C}^{B})^{t+\Delta t}$ is positive definite), we can obtain the following inequality

$$\|\mathbf{v}^{t+\Delta t,m}\|_2<\|\mathbf{v}^{t+\Delta t,m-1}\|_2 \quad (16)$$

if the following condition is satisfied1:

$$0<\alpha<\frac{2}{\lambda_{max}} \quad (17)$$

where λ_{max} is the maximum eigenvalue of matrix $(\mathbf{C}^{A}+\mathbf{C}^{B})^{t+\Delta t}$.

3.3 Practical considerations

In the actual computation, for computing α, $\|(\mathbf{C}^{A}+\mathbf{C}^{B})^{t+\Delta t}\|_\infty$ may be used instead of λ_{max} because $\|(\mathbf{C}^{A}+\mathbf{C}^{B})^{t+\Delta t}\|_\infty$ is conveniently computed by considering the maximum displacement change due to a unit force at a suitable contact point. Thus, in this work, the value of α in the iterative scheme of Eq. (6) is given by the following :

$$\alpha=\frac{1.9}{\|(\mathbf{C}^{A}+\mathbf{C}^{B})^{t+\Delta t}\|_\infty} \quad (18)$$

However, if the conditions of equation (11) are not satisfied, sometimes $\|\mathbf{v}^{t+\Delta t,m}\|_2$ may not become smaller than $\|\mathbf{v}^{t+\Delta t,m-1}\|_2$ by iterative scheme given by Eq. (6) using the above value of α. In such cases, in the practical computation, the mth iteration repeated again by consecutively reducing the value of α to half until $\|\mathbf{v}^{t+\Delta t,m}\|_2$ becomes smaller than $\|\mathbf{v}^{t+\Delta t,m-1}\|_2$. It is worth to note that all the conditions of Eq. (11) are satisfied if the value of α is small. Also, for an efficient computation, even though the solution acceleration technique of Lee (1989) is not employed in this work, penalty methods may be efficiently employed on the points where it is absolutely clear that normal contact or tangential sticking will occur for example, by checking the variations of the contact forces during the recent consecutive time steps, if it is judged that some points will not be separated in the current time step or if sticking will occur in the tangential direction on some points in the current time step, then the corresponding contact constraints may be efficiently imposed by using the penalty terms.

3.4 Implementation to ABAQUS and computation procedure

To solve the nonlinear global equilibrium

equations by the finite element method, at each iteration of Newton Raphson method, the stiffness matrix and the force vector should be computed for each element. Also ABAQUS provides a user subroutine, UEL, to compute the stiffness matrix and the force vector of a user-defined element. This work uses ABAQUS for general computations of the finite element method, and the computation to impose the contact conditions on the possible contact points are implemented to ABAQUS by using the UEL subroutine. Even though all the computations for ordinary finite element procedures except the contact analysis are done by ABAQUS, the contact conditions are imposed by using the user subroutine UEL instead of the ABAQUS input file. Howerer subroutine UEL of ABAQUS is basically used for computing the stiffness matrix and the force vector of a user-defined element at each iteration of the Newton Raphson method. Thus additional considerations are required to perform the computations for the contact analysis in subroutine UEL. To impose the contact constraints by using UEL, the nodal points of a user-defined element contains an artificial nodal point which does not exist in the real material as well as the real nodal points existing on the possible contact surfaces. The artificial nodal point is introduced in a user-defined element to perform all the computations required for the contact analysis suggested in this work.

To solve the global nonlinear equilibrium equations, ABAQUS calls the UEL subroutine at each iteration of the Newton Raphson method. Also, to solve the contact problems by the present technique, the global nonlinear equations should be solved by the Newton Raphson method whenever the contact force is iteratively modified by equation (6). Since the Newton Raphson method of the global nonlinear equations of ABAQUS should proceed with a monotone reduction of the global unbalanced force vector, the unbalanced force corresponding to the artificial nodal point is given an extremely high value at the first Newton Raphson iteration of each time step, in subrautine UEL of the user-defined element and it is artificially diminished to smaller values at the subsequent iterations of the Newton Raphson method. Simultaneously, whenever UEL is called by ABAQUS, the convergence of Newton Raphson iterations of the global nonlinear equations with the prescribed contact forces is checked by using the variations of the displacements of the real nodal points of the user-defined element. If the convergence criterion for Newton Raphson method is satisfied, the contact error vector is computed by equation (3) or (7) and the contact force is computed by equation (6). Finally, if the convergence criterion of iterative scheme of equation (6) is satisfied (e.g., if the magnitude of contact error vector of equation (3) or (7) becomes smaller than the prescribed tolerance), the artificial unbalanced force at the artificial nodal point is set to be zero. By this way, it is possible to solve the global equilibrium equation with the correct contact force. Also, in subroutine UEL, the normal and tangential contact forces on the real contact points are transformed to the nodal forces of the global equations, If penalty method is used on some contact points, the corresponding stiffness matrices and force vectors are also computed in subroutine UEL. Besides the important computations mentioned above, all the other computations for contact analysis such as detecting the positions and normal directions of the contact pairing points should also be performed in subroutine UEL, and thus the computation procedure is rather complicated. The computation procedure at time step $t+\Delta t$ is schematically summarized below.

1. Set $m=0$. Initialize the contact pairing points and the normal directions by using the geometries of the possible contact surfaces of the previous time step, and initialize $\mathbf{p}^{t+\Delta t,0}$, $\tau^{t+\Delta t}$, and the contact points where penalty method may be applied. Go to step 4.
2. If $m=1$, change $\mathbf{p}^{t+\Delta t,1}$ by increasing a unit force on the point which is suitable for computing $\|(\mathbf{C}^A+\mathbf{C}^B)^{t+\Delta t}\|_\infty$, and go to step 4. If $m=2$, compute α by equation (18), and go to step 3.
3. If $m\geq 2$, compute $\mathbf{p}^{t+\Delta t,m}$ by iterative scheme of equation (6) (especially, if $m=2$, on the right hand side of iterative scheme of equa-

tion (6), use the contact force and contact error vector at m=0).

4. Compute the displacement (and velocity in case of dynamics problems) by solving the global equilibrium equations by the Newton Raphson iterations of ABAQUS. Check if the Newton Raphson method of ABAQUS converges or not. As only subroutine UEL is used for the contact analysis in this work, the convergence of the global equilibrium equations of ABAQUS is indirectly checked by observing the variations of the nodal displacements of the user-defined element. For example, let $\delta\mathbf{u}$ be the increment of displacements during the consecutive Newton Raphson iterations, and let $\Delta\mathbf{u}$ be the total increment of the displacements in time step $t+\Delta t$. Then the convergence is assumed to be satisfied if $\| \delta\mathbf{u} \|_2/\| \Delta\mathbf{u} \|_2$ becomes smaller than the prescribed tolerance. If the Newton Raphson method converges, go to step 5. Otherwise, repeat the iteration until the convergence of the global equilibrium equation is obtained.
5. If m=1, go to step 2 with m=m+1. Otherwise, go to step 6.
6. Determine the contact pairing points and the normal directions by drawing the normal lines from the nodal points on the possible contact surface of a body to the possible contact surface of the other body. If m≠0, compute the error vector $\mathbf{v}^{t+\Delta t,m}$ by definition give by equation (3) or (7), and go to step 7. If m=0, after computing $\mathbf{v}^{t+\Delta t,m}$, go to step 2 with m=m+1.
7. If $\tau^{t+\Delta t}$ or the contact points for penalty method were revised at the (m−1)th iteration, go to step 3 with m=m+1. Otherwise, go to step 8.
8. If $\| \mathbf{v}^{t+\Delta t,m} \|_2 < \| \mathbf{v}^{t+\Delta t,m-1} \|_2$ (in case of m=2, if $\| \mathbf{v}^{t+\Delta t,2} \|_2 < \| \mathbf{v}^{t+\Delta t,0} \|_2$), go to step 9. Otherwise, go to step 3 with $\alpha=\alpha/2$ to repeat the computation of the mth iteration.
9. At the specified iteration (e.g., at the iteration where $\| \mathbf{v}^{t+\Delta t,m} \|_2$ is reduced to less than 10% of $\| \mathbf{v}^{t+\Delta t,0} \|_2$), revise $\tau^{t+\Delta t}$ and the contact points where penalty methods are applied (if necessary, revise α by equation (18) with the currently computed contact points), and go to step 3 with m=m+1. Otherwise, go to step 10.
10. If $\| \mathbf{v}^{t+\Delta t,m} \|_2$ is smaller than the prescribed tolerance, go to step 11. Otherwise, go to step 3 with m=m+1.
11. Check if $\tau_i^{t+\Delta t} - \mu | \mathbf{p}_i^{t+\Delta t,m-1} |$ is within the specified tolerance on each contact point i. Also, check the contact errors on the contact points where computation was done with the penalty methods. If the errors are within the prescribed tolerances, terminate the computation of this time step, and go for the next time step. Otherwise, revise $\tau^{t+\Delta t}$ and the contact points where penalty methods are applied (if necessary, revise α by equation (18) with the currently computed contact points), and go to step 3 with m=m+1.

4. Numerical Examples

4.1 Computation with Model 1

The two-dimensional solids shown in Fig. 1 are considered here. Body A is a narrow rectangle whose length and height are 12 and 0.4 cm, respectively. The upper and lower surfaces of body B are circles whose radii are 10 cm and 8.5 cm, respectively. The left sides of both bodies are fixed as shown in Fig. 1, and there is a clearance

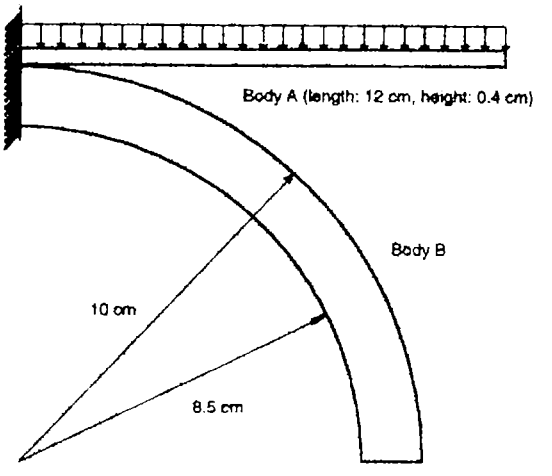

Fig. 1 Model for the statics problem

of 0.05 cm between the lower left corner of body A and the upper left corner of body B. Each body is modeled by 600 four-node plane stress elements (6 rows along the width and 100 rows along the length). The friction coefficient is taken to be 0.3. For comparison the contact analysis is performed twice by ABAQUS (2001) using the Lagrange multiplier method and by the present technique. In the present contact analysis technique, for each contact point on the slave surface, the master contact surface is locally smoothed by using Lagrange interpolations connecting the nearest four nodal points. Firstly, the materials are assumed to be elastic with Young's modulus of 200 GPa and Poisson's ratio of 0.3. A uniform external pressure of 50 MPa is assumed to be applied on the upper surface of body A. Figure 2 shows that, in the ABAQUS solutions, even though severe oscillations develop if 40% of the contact segments are smoothed to parabolic curves with the default value of 0.2 for parameter SMOOTH, smooth contact stress distributions can be obtained if 100% of the segments are smoothed to parabolic curves with SMOOTH=0.5. This result is similar to those of El-Abbasi et. al. (2001) and Wriggers et. al (2001) where the effects of smoothed contact surfaces are demonstrated. Figure 2 also shows that the contact stress distributions obtained by the present technique are smooth. Secondly, the materials are assumed to be elastic-plastic. Young's modulus is 200 GPa, Poisson's ratio is 0.3, yield stress is 170 MPa, and strain beyond the yieldins point is given $\epsilon=(\sigma/K)^n$ with K=0.510 GPa and n=4.76.

A uniform external pressure of 3.5 MPa is assumed to be applied on the upper surface of body A. Then, as shown in Fig. 3, even if 100% of the contact segments are smoothed with SMOOTH=0.5, severe oscillations develop in the ABAQUS contact stress distributions. Even though the ABAQUS solution may be further smoothed by assuming a softened contact, then the solution accuracy may be lost by the softening or it is very difficult to guess the suitable values for the softening data before the solution. For this specific model, among the solutions obtained by several trials, the best one which contains minor oscillations seems to be obtained with $c=10^{-4}$ cm and $p^0=40$ MPa as ABAQUS softening data, and is shown in Fig. 3. In this ABAQUS solution the contact pressure is assumed to increase from zero to p^0 when the normal clearance between the contact surfaces is reduced from c to zero. Figure 3 shows that the contact stress distribution obtained by the present technique is smoother than the ABAQUS solution even when the softened contact assumption is adopted. In Figs. 2 and 3, similar to the results of El-Abbasi et. al. (2001), the peak contact stresses develop on both ends of the contact region. These peak contact stresses can be explained

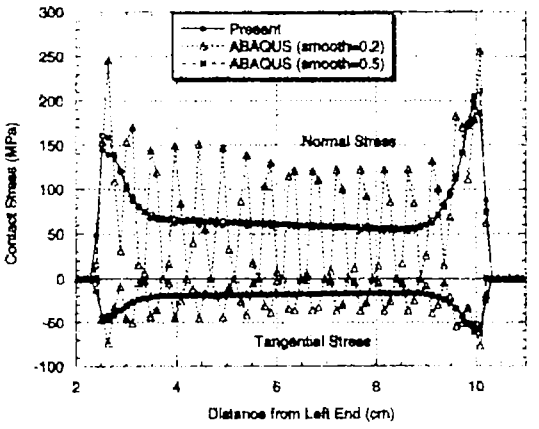

Fig. 2 Comparison of contact stress distributions of elastic case

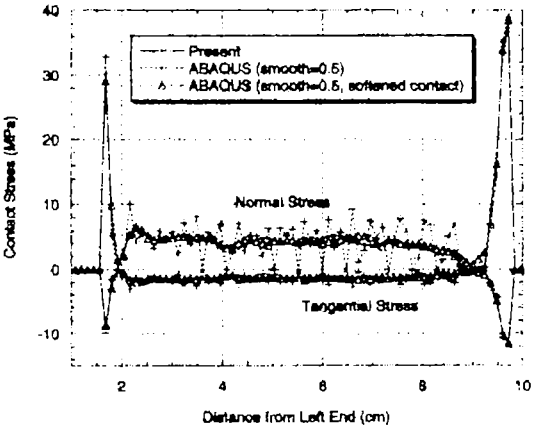

Fig. 3 Comparison of contact stress distributions of elastic-plastic case

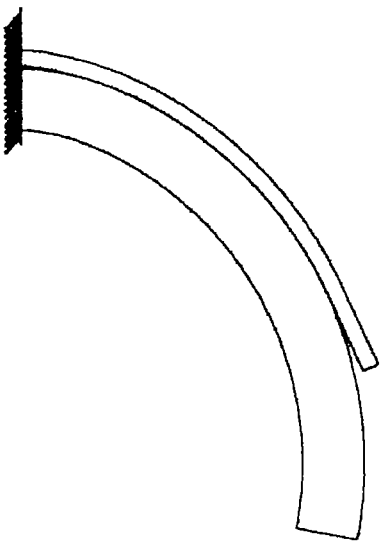

Fig. 4 Deformed shape of the model

by considering the shear force equilibrium equations from the contact-end point to the rest of the beam. The deformed shape of the elastic-plastic model is shown in Fig. 4.

4.2 Computation with Model 2

In the second model a heavy elastic wheel moves on the elastic beam from the left end as shown in Fig. 5. This model is employed to compare the solution with that of Vu-Quoc (1989) where a rigid wheel traversing an elastic beam is solved. It is worth to note that, besides the high-speed rotation of the wheel surface, the beam upper surface also rotates due to the beam deflection. The circular wheel is modeled by 90 plane stress elements (3 rows along the radial direction, and 30 rows along the circumferential direction), and the beam is modeled by 300 four-node plane stress elements (6 rows along the height and 50 rows along the length). The beam is simply supported as shown in Fig. 5. The data for the wheel are : radius of the circle is 1 m, Young's modulus is 100 GPa, Poisson's ratio is 0.3, total weight is 3000 kg , and the initial horizontal velocity is 100 m/s. The data for the beam are : length is 24 m, height is 0.6 m, width is 1 m, Young's modulus is 55.6 GPa, Poisson's ratio is 0., and density is 2083.4 kg/m^3. Thus, the

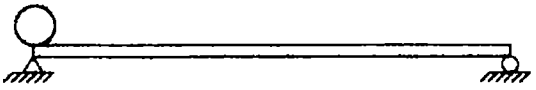

Fig. 5 Model for the dynamics problem

bending rigidity, EI, and the mass of the beam as well as the wheel mass are the same as those of Vu-Quoc (1989). The vertical force of 600 kN is applied on the wheel, and friction coefficient between the wheel and the beam is assumed to be 0.3. For this model, even though local Hertzian elastic deformation occurs on the contact surfaces between the elastic wheel and the beam, such local Hertzian deformation is negligible compared to the global deformation of the whole structure. Also, by the Hertzian contact theory (Timoshenko, 1970), the length of the real contact region occurring between the elastic wheel and the flat surface is calculated to be much smaller than the element length on the contact surface. By these reasons, the contact region of this model may be represented by a point (i.e., point-to-point contact) neglecting the local Hertzian deformation. In this work, the outer surface of the rotating wheel and the beam upper surface are represented by cubic spline interpolations, and the contact point between the two surfaces are detected by computing the minimum normal distance. Thus, the contact point need not be a nodal point. Then the contact constraint error and the contact force were computed by using the theory of this work, and the variation of the contact force is shown in Figure 6. As the initial angular velocity of the wheel is assumed to be zero, the wheel slides on the beam surface in the beginning and its angular velocity gradually increases to 31.4 rad/sec by friction on the beam. Fig. 6 shows that, even though the total traversing time slightly increases due to the sliding friction, the contact force variation is almost similar to that of Vu-Quoc (1989). For reference the normal contact force variation of this model computed by the ABAQUS/Standard is also shown in Figure 7. In the ABAQUS solution of Fig. 7, the contact force oscillates even with positive and negative values, and it is apparent that this kind of model cannot be computed with the node-to-segment contact

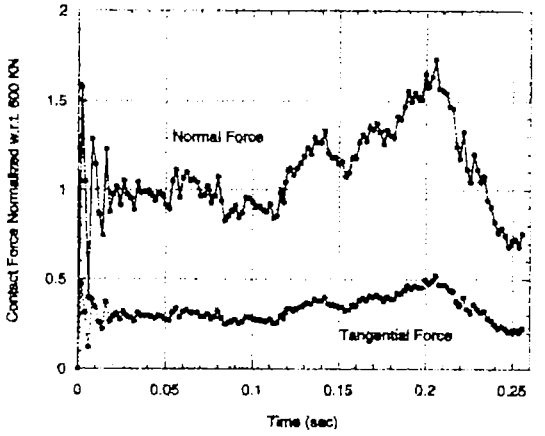

Fig. 6 Variation of normal and tangential contact forces by the present technique

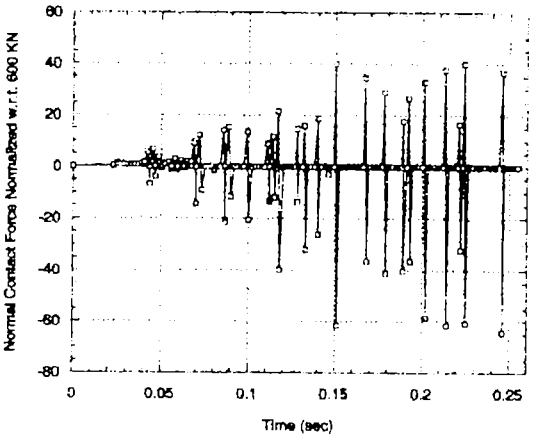

Fig. 7 Variation of normal contact force by ABAQUS

strategy which is employed in most of the commercial FEM codes including ABAQUS. Here the solutions were time integrated by Hilber-Hughes-Taylor scheme with the maximum time step size of 0.005 sec, and β and γ of equation (7) were selected as 1/3 and 1/6, respectively. Even though the present solution is insensitive to the values of β and γ as demonstrated by Lee(2002), if equal weights should be considered for the displacement, velocity, and acceleration, β and γ may be selected as 1/3 and 1/6, respectively, because of the relation $(\mathbf{s}^{t+\Delta t,m}-\mathbf{s}^{t+\Delta t,m-1}) \approx (\dot{\mathbf{s}}^{t+\Delta t,m}-\dot{\mathbf{s}}^{t+\Delta t,m-1})\Delta t/3 \approx (\ddot{\mathbf{s}}^{t+\Delta t,m}-\ddot{\mathbf{s}}^{t+\Delta t,m-1})\Delta t^2/6$.

5. Conclusion

The contact conditions have been systematically expressed by the contact error and the associated iterative technique has been employed to reduce the contact error with the normal directions computed at each iteration on the rotating contact surface. Furthermore, the present contact analysis technique has been implemented to ABAQUS by employing the UEL user subroutine. The numerical experiments show that almost smooth contact solution is possible by the present technique. For the dynamic contact, the contact condition has also been expressed by defining a single contact error combining the displacement, velocity, and acceleration on each contact point, and the same iterative method has been used to reduce the contact error vector monotonically toward zero. The computed results indicate that, even when severe spurious oscillations occur in the ABAQUS solution, almost smooth and correct solution is possible by the present technique.

Acknowledgement

This work was supported by Korea Research Foundation (KRF-99-041-E00034).

References

ABAQUS Manual, Hibbit, Karlsson & Sorensen, Inc., Version 6.2, 2001.

Bathe, K. J. and Chaudhary, A. B., 1986, "A Solution Method for Static and Dynamic Analysis of Three-Dimensional Contact Problems with Friction," *Comput. Struct.* Vol. 24, pp. 855~873.

Crisfield, M. A., 1997, *Non-linear Finite Element Analysis of Solids and Structures*, Vol. 2, John Wiley and Sons, Chichester.

El-Abbasi, N., Meguid, S. A. and Czekanski, A., 2001, "On the Modeling of Smooth Contact Surfaces Using Cubic Splines," *Int. J. Numer. Method Engng.*, Vol. 50, pp. 953~967.

Ghosh, S., 1992, "Arbitrary Lagrangian-Eu-

lerian Finite Element Analysis of Large Deformation in Contacting Bodies," *Int. J. Numer. Method Engng.*, Vol. 33, pp. 1891~1925.

Heegaard, J. H. and Curnier, A., 1993, "An Augmented Lagrangian Method for Discrete Large-Slip Contact Problems.," *Int. J. Numer. Method Engng.*, Vol. 36, pp. 569~593.

Hughes, T. J. R., Taylor, R. L., Sackman, J. L., Curnier, A., and Kanoknukulchai, W., 1976, "A Finite Element Method for a Class of Contact-Impact Problem," *Comput. Method Appl. Mech. Engng.*, Vol. 8, pp. 249~276.

Laursen, T. A. and Simo, J. C., 1993, "A Continuum-Based Finite Element Formulation for the Implicit Solution of Multibody Large Deformation Frictional Contact Problems," *Int. J. Numer. Method Engng.*, Vol. 36, pp. 3451~3485.

Lee, K., 1989, "An Efficient Solution Method for Frictional Contact Problems," *Comput. Struct.*, Vol. 32, pp. 1~11.

Lee, K., 1994, "A Numerical Solution for Dynamic Contact Problems Satisfying the Velocity and Acceleration Compatibilities on the Contact Surface," *Computational Mechanics*, Vol. 15, pp. 189~200.

Lee, K., 1997, "A Numerical Method for Dynamic Analysis of Vehicles Moving on Flexible Structures Having Gaps," *Int. J. Numer. Method Engng.*, Vol. 40, pp. 511~531.

Lee, K., 2002, "Numerical Analysis of Dynamic Contact with Combined Constraint of Displacement, Velocity and Acceleration on the Contact Surface," *Proc. Instn. Mech. Engrs, Part C, Journal of Mechanical Engineering Science*, Vol. 216, pp. 377~382.

Petzold, L., 1982, "Differential Algebraic Equations Are Not ODEs," *SIAM. J. Sci. Stat. Comput.*, Vol. 3, pp. 367~384.

Taylor, R. L. and Papadopoulos, P., 1993, "On a Finite Element Method for Dynamic Contact/Impact problems," *Int. J. Numer. Method Engng.*, Vol. 36, pp. 2123~2140.

Timoshenko, S. P. and Goodier, J. N., 1970, *Theory of Elasticity*, McGraw-Hill, New York.

Vu-Quoc, L. and Olsson, M., 1989, "A Computational Procedure for Interaction of High-Speed Vehicles on Flexible Structures Without Assuming Known Vehicle Nominal Motion," *Comput. Meth. Appl. Mech. Engng.*, Vol. 76, pp. 207~244.

Wriggers, P., Krstulovic-Opara, L. and Korelc, J., 2001, "Smooth C^1-Interpolations for Two-Dimensional Frictional Contact Problems," *Int. J. Numer. Method Engng.*, Vol. 51, pp. 1469~1495.